A Novel Synthesis Technique for Conducting Scatterers Using TLM Time Reversal

Michel Forest and Wolfgang J. R. Hoefer, *Fellow, IEEE*

***Abstract*—This paper presents a novel numerical synthesis technique based on the reversal of the TLM process in time. It allows the designer to generate the geometry of a passive structure from its desired frequency response using alternate forward and backward time domain simulations. The essential steps of the procedure are explained and validated using, as an example, the synthesis of an inductive obstacle in a waveguide. If fully developed, it promises to become an advantageous alternative to the traditional techniques using frequency domain numerical methods.**

I. Introduction

DESIGN of microwave structures through repeated analyses combined with an optimization strategy has been performed extensively for many years and is growing with the increasing capability of computers. Depending on the nature of the problem, a large number of analysis cycles are necessary to achieve satisfactory convergence of the design process. Although these methods demonstrate very good performance in the frequency domain, those successive analyses would be very wasteful in the time domain since each analysis requires the transient build-up of the field from an impulsive excitation. Thus, when using a time domain method, a completely different approach should be taken that makes appropriate use of the time dimension. The principles of a new technique based on time reversal have been recently introduced by Sorrentino *et al.* [1]. This new procedure amounts to a time domain synthesis of microwave structures with the Transmission-Line Matrix method (TLM).

The main advantage of a time domain method resides in the ability to work with a large bandwidth signal and the possibility to include transient phenomena which are both important in the time domain synthesis of a microwave structure. In this paper, the new synthesis procedure will be described in detail and applied to a simple example so as to not obscure the essence of the method by the complexity of the structure. Finally, results will be discussed and compared with existing design methods.

II. Reversibility of Time in the TLM Method

The Transmission-Line Matrix (TLM) method was first introduced by Johns and Beurle [2]. It is a discrete time and space sampling method for modeling the propagation of electromagnetic waves. The propagation space is represented by a mesh of interconnected transmission lines. The well-known two-dimensional TLM shunt node is represented schematically in Fig. 1.

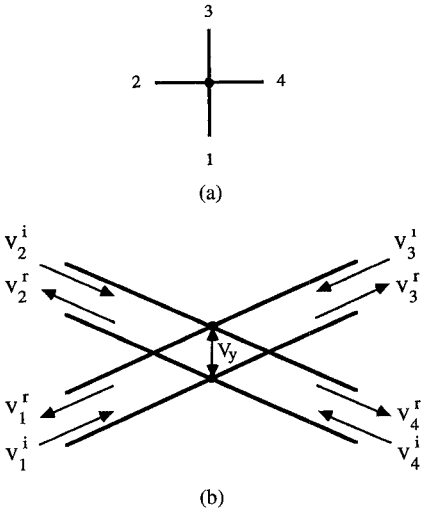

Fig. 1. 2D-TLM shunt node. (a) Schematic. (b) Three-dimensional view.

For two-dimensional homogeneous regions, the voltage impulses V_n^i incident on each line are scattered according to the node scattering matrix

$$\begin{bmatrix} V_1 \\ V_2 \\ V_3 \\ V_4 \end{bmatrix}^r_{k+1} = \frac{1}{2}\begin{bmatrix} -1 & 1 & 1 & 1 \\ 1 & -1 & 1 & 1 \\ 1 & 1 & -1 & 1 \\ 1 & 1 & 1 & -1 \end{bmatrix}\begin{bmatrix} V_1 \\ V_2 \\ V_3 \\ V_4 \end{bmatrix}^i_k. \tag{1}$$

Furthermore, each scattered impulse V_n^r at a given node becomes an incident impulse V_n^i at the adjacent node. The total node voltage V_y at the instant of scattering is

$$V_y = \frac{1}{2}\sum_{n=1}^{4} V_n^i. \tag{2}$$

It has been shown in [1] that the TLM process is reversible due to the fact that the scattering matrix is equal to its inverse

$$S^{-1} = S \tag{3}$$

where

$$S = \frac{1}{2}\begin{bmatrix} -1 & 1 & 1 & 1 \\ 1 & -1 & 1 & 1 \\ 1 & 1 & -1 & 1 \\ 1 & 1 & 1 & -1 \end{bmatrix}. \tag{4}$$

Manuscript received January 26, 1993; revised September 28, 1994. This work was supported by the Natural Sciences and Engineering Research Council of Canada.

M. Forest is with the Space Systems Division, Spar Aerospace Ltd., Sainte-Anne-de-Bellevue, P.Q., Canada H9X 3R2.

W. J. R. Hoefer is with the Department of Electrical and Computer Engineering, University of Victoria, Victoria, B.C., Canada V8W 3P6.

IEEE Log Number 9410693.

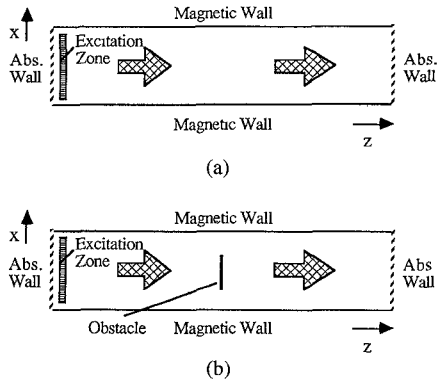

Fig. 2. Parallel plate waveguide. (a) Waveguide with an obstacle yielding the total field solution. (b) Empty waveguide yielding the homogeneous field solution.

This property of the TLM scattering matrix implies that by reversing the process without changing the algorithm, one can reconstruct a source distribution from a known field solution by reversing the TLM process in time. This is also true for the three-dimensional distributed and condensed node algorithms. An extensive list of references on these algorithms is given in [3]. Other workers such as Bennet [4] have also worked on time domain inverse problems. However, their work is rather based on a space–time integral equation approach.

III. Reconstruction Technique Using Time Reversal

The essence of the time reversal synthesis will be explained and demonstrated for the reconstruction of a simple discontinuity—a thin conducting obstacle—in a parallel plate waveguide. This guide can propagate a TEM wave, and it possesses a complete spectrum of well-defined modes.

Fig. 2 shows the parallel plate waveguide without (a) and with (b) the obstacle. Both structures are terminated at both ends by an absorbing boundary (generated by zero reflection coefficients on the output lines) and excited in the linear excitation zone by a Gaussian impulse, a signal with a limited bandwidth such that the traveling waveform is not noticeably distorted due to velocity dispersion. The obstacle is a conducting septum consisting of an electric wall inserted into the center of the parallel plate waveguide. The following procedure consists of three stages.

1) Forward analysis of the empty waveguide to obtain the homogeneous field solution in the empty waveguide.

2) Forward analysis of the loaded waveguide to obtain the total field solution which is the sum of the homogeneous solution and the scattered field (particular solution).

3) Backward synthesis to reconstruct the topology of the scattering obstacle.

In the first stage, a time-sampled Gaussian impulse is injected into the empty waveguide section, and the resultant impulses incident upon both absorbing boundaries are picked up and stored. We refer to these impulses at each boundary node as $\phi^H_{\text{left}}(i, k)$ and $\phi^H_{\text{right}}(i, k)$. The index "$i$" indicates the position in the transversal direction, "k" represents the discrete time step, and "H" refers to the homogeneous solution.

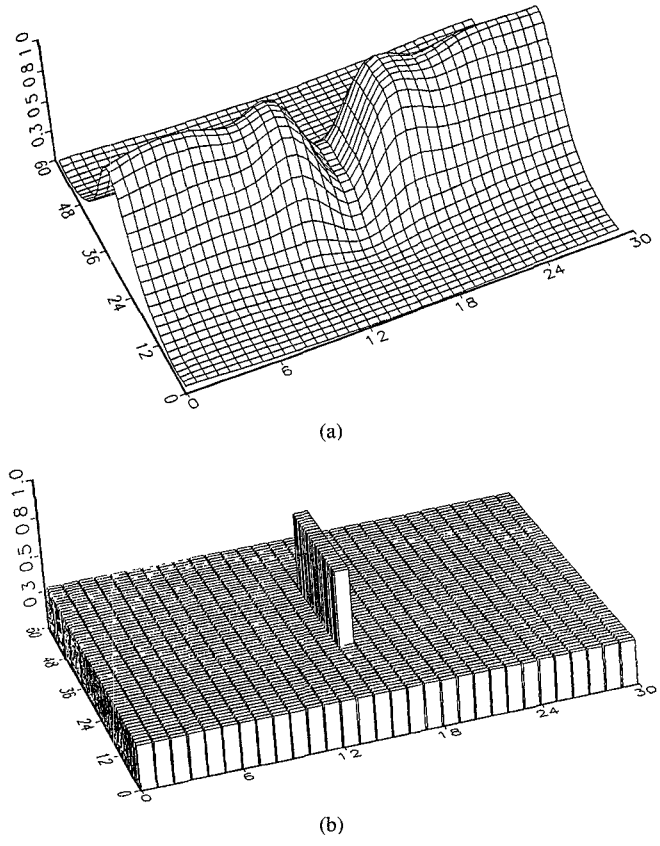

Fig. 3. Results for the synthesis of a metallic septum. (a) Distribution of the maximum value of the magnitude of the Poynting vector inside the structure after the inversion of the TLM process. (b) Shape of the reconstructed obstacle extracted from the Poynting vector distribution.

In the second stage, the same function is stored with the discontinuity in place, yielding the impulse responses $\phi^T_{\text{left}}(i, k)$ and $\phi^T_{\text{right}}(i, k)$, the total field solution. Note that the number "k" of time steps must be the same in both cases. Finally, in the third stage, both impulse responses are subtracted from each other as follows, yielding the particular solutions

$$\phi^P_{\text{left}}(i, k) = \phi^T_{\text{left}}(i, k) - \phi^H_{\text{left}}(i, k) \tag{5}$$

and

$$\phi^P_{\text{right}}(i, k) = \phi^T_{\text{right}}(i, k) - \phi^H_{\text{right}}(i, k). \tag{6}$$

These functions are then injected in the reverse time sequence at both ends of the empty waveguide. The same number of computation (or time) steps is performed as in the forward simulations. Note that for the analysis, the number of time steps must be large enough to let the field vanish completely in the waveguide because it is assumed that there is no field in it when the inverse simulation is started.

At each computational step of the synthesis, the absolute value of a field component, for example, E_y, is displayed at each node inside the structure according to a color map, and updated if the new value is larger than the maximum value at any previous time step. Therefore, the final picture of the distribution of the fields represents the maximum value that occurred at each node during the entire reverse process. In

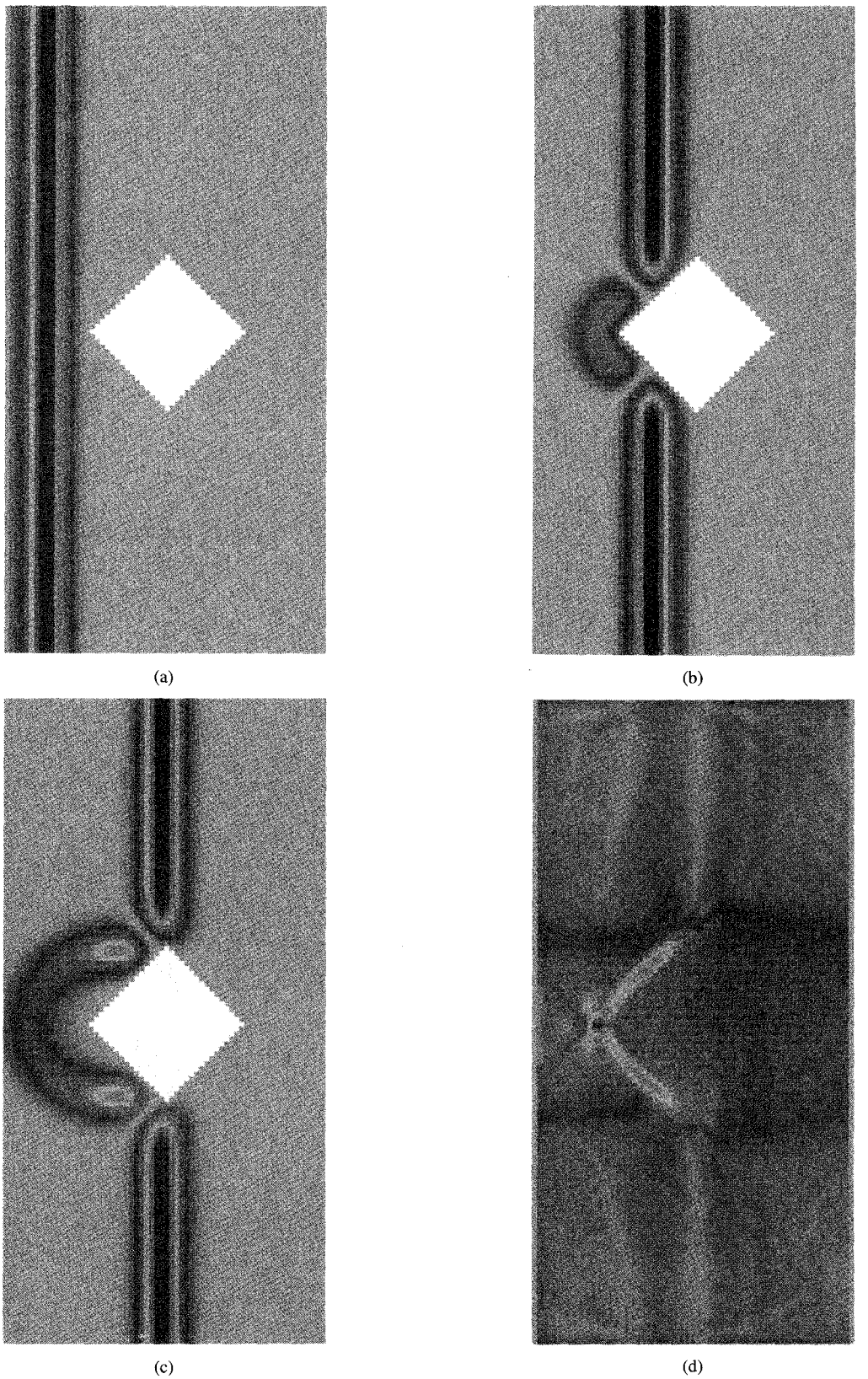

Fig. 4. Results for the synthesis of a metallic scatterer. (a) TLM simulation: Part 1. (b) TLM simulation: Part 2. (c) TLM simulation: Part 3. (d) Distribution of the maximum electric field. These figures show the absolute value of the electric field normal to the plates (E_y). (a), (b), and (c) show parts of the forward simulation to obtain the total field solution. (d) shows the results of the reverse simulation with the distribution of the maximum value of the electric field into the structure. The highest points indicate the location of the induced sources on the contour of the obstacle.

this manner, the shape of the obstacle can be reconstructed. To explain why only the maximum field value over time should be taken to do the imaging, remember that there is no obstacle in the guide when the particular solutions

are launched, and therefore the field components will have vanished completely at the end of the reverse process. The different field components will show different aspects of the contour of the obstacle. For instance, the highest values of the normal electric field occur at the surface of the obstacle, and so do the lowest values of the normal magnetic field. Also, the longitudinal magnetic field component can be used to indicate the positions of the sharp edges of the scatterer. Furthermore, it is possible to define the obstacle contour with better precision using a combination of these field components. For example, the magnitude of the Poynting vector can be used, which is computed as follows:

$$|P(i, j)| = |E_y(i, j)|\sqrt{|H_x(i, j)|^2 + |H_z(i, j)|^2} \quad (7)$$

where the indexes "i" and "j" specify the position in the waveguide. As an example, Fig. 3(a) shows the final image from which the conducting septum is reconstructed. The valley formed in the distribution of the maximum magnitude of the Poynting vector describes the location and the shape of the septum. A simple algorithm is used to extract the position of this valley in order to determine the shape of the obstacle. Fig. 3(b) shows the image of the reconstructed obstacle, which can be obtained with a resolution corresponding to the mesh parameter Δl.

Fig. 4 shows a sequence of images including both the forward and backward analyses of a diamond-shaped conducting obstacle. In Fig. 4(a), (b), and (c), three different time steps of the forward analysis are displayed. The Gaussian-shaped traveling wave is excited at the left port and is propagating to the right side of the guide. Throughout the simulation, all impulses emerging at both ends of the waveguide are stored in memory. The distribution of the maximum value of the magnitude of the electric field in the structure is presented in Fig. 4(d). The left side of the obstacle is indicated by the locations of the larger electric field values. It corresponds to the location of the induced sources on the contour of the metallic obstacle.

These examples demonstrate the simplicity of the reconstruction of metallic scatterers by inversion of the TLM process in time. Obviously, the resolution depends on the relative density of the mesh and the resulting resolution of the Gaussian excitation waveform.

IV. Complete Synthesis Procedure

A realistic synthesis does not start with an analysis of the desired structure as in the previous demonstration, but rather from a desired time or frequency response, the latter being the more frequently encountered case. However, such a frequency response usually does not contain information for frequencies considerably higher than the upper band limit of interest. For example, the specifications for an inductive iris are given only for the dominant mode, and there is no information about the distribution of energy among the different higher order modes. In other words, there is no information about the transversal distribution of the fields in the reference planes. Nevertheless, this information is essential for the reconstruction of the obstacle in the time domain.

Hence, this missing information must be obtained somehow. As in the traditional synthesis techniques which involve optimization procedures, a first guess is used as a starting point. This is, in fact, a simple way to generate the missing information approximately. A first forward TLM analysis is performed of an obstacle having approximately the desired dimensions. These can be found in many cases from closed-form expressions, given in the literature, which link the dimensions of discontinuities to their equivalent lumped element circuits. However, if such expressions are not available, an educated guess is sufficient. The dominant mode content of this first response $\phi^T_{\text{left}}(i, k)$ and $\phi^T_{\text{right}}(i, k)$ is extracted and replaced by the desired dominant mode content in the frequency domain. The modified total response is then converted back into the time domain and, after subtraction of the homogeneous response of the empty waveguide, reinjected into the computational domain in the inverse time sequence. This procedure will now be described in more detail.

A. Modification of the Dominant Mode Response of a Structure

An important part of the TLM synthesis of microwave structures is the modification of the dominant mode information provided by an approximated analysis. In this manner, the reinjected signal will yield a structure which has the desired frequency response within the single mode bandwidth.

Let the time domain responses for the electric field of the approximated structure be $\phi^T_{\text{left}}(i, k)$ and $\phi^T_{\text{right}}(i, k)$. From these signals, the dominant mode frequency response is extracted by performing a spatial Fourier expansion in the transverse (x) direction of the waveguide at every iteration, and then taking the Fourier transform of the resulting time sequence. In the case of the parallel plate waveguide (see Fig. 2), the TEM mode has a constant transversal distribution. Thus, the extraction of the dominant mode for each iteration is performed by taking the first term of the transverse Fourier spatial expansion of the electric field along x

$$\phi^D_{\text{left}}(k) = \frac{1}{NBX}\sum_{i=1}^{NBX}\phi^T_{\text{left}}(i, k) \quad (8)$$

and

$$\phi^D_{\text{right}}(k) = \frac{1}{NBX}\sum_{i=1}^{NBX}\phi^T_{\text{right}}(i, k) \quad (9)$$

for $k = 0, 1, 2\cdots NbIt- 1$ where NBX and $NbIt$ are, respectively, the number of nodes in the transverse direction and the number of time steps during the analysis.

Then $\Phi^D_{\text{left}}(\omega)$ and $\Phi^D_{\text{right}}(\omega)$ are obtained using a discrete Fourier transform (DFT) on $\phi^D_{\text{left}}(k)$ and $\phi^D_{\text{right}}(k)$. It is important to note that ϕ^D_{left} contains the incident and the reflected TEM wave, while ϕ^D_{right} contains only the transmitted TEM wave.

Let the desired frequency responses be $\Phi^W_{\text{left}}(\omega)$ and $\Phi^W_{\text{right}}(\omega)$ which are defined in a limited frequency band where only the dominant mode can propagate.—Note that only the magnitude of the S parameter is used here. The effect of the phase has not been evaluated.—The difference

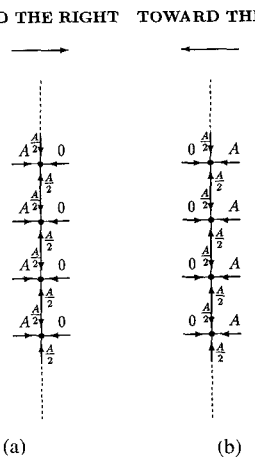

Fig. 5. Representation of a TEM wave traveling (a) to the right and (b) to the left. The magnitude of the electric field of the wave is unity in both cases.

between these and the previous signals is performed in the frequency domain, yielding

$$\Phi^{\text{diff}}_{\text{left}}(\omega) = \Phi^{D}_{\text{left}}(\omega) - \Phi^{W}_{\text{left}}(\omega) \tag{10}$$

and

$$\Phi^{\text{diff}}_{\text{right}}(\omega) = \Phi^{D}_{\text{right}}(\omega) - \Phi^{W}_{\text{right}}(\omega). \tag{11}$$

Since $\Phi^{D}(\omega)$ and $\Phi^{W}(\omega)$ have the same incident field content, the above difference signals [in (10) and (11)] contain a reflected and a transmitted TEM wave, respectively, which have a constant transversal distribution in the waveguide. Uniform TEM waves are represented in Fig. 5 where the impulses V_i incident on a transversal row of nodes are indicated for a given time step. For the wave traveling to the left, the field components are calculated as follows:

$$\begin{aligned} E_y &= \frac{1}{2}\sum_i V_i \\ &= \frac{1}{2}\left[\frac{1}{2} + 0 + \frac{1}{2} + 1\right] \\ &= 1, \end{aligned} \tag{12}$$

$$\begin{aligned} H_x &= \frac{1}{Z_0}(V_4 - V_2) \\ &= \frac{1}{Z_0}(1 - 0) \\ &= \frac{1}{Z_0}, \end{aligned} \tag{13}$$

$$\begin{aligned} H_z &= \frac{1}{Z_0}(V_1 - V_3) \\ &= \frac{1}{Z_0}\left(\frac{1}{2} - \frac{1}{2}\right) \\ &= 0. \end{aligned} \tag{14}$$

These expressions verify that the Poynting vector is effectively directed in the negative z direction, which is the direction of propagation. For a TEM wave traveling to the right, we have

$$\begin{aligned} E_y &= \frac{1}{2}\sum_i V_i \\ &= \frac{1}{2}\left[\frac{1}{2} + 1 + \frac{1}{2} + 0\right] \\ &= 1, \end{aligned} \tag{15}$$

$$\begin{aligned} H_x &= \frac{1}{Z_0}(V_4 - V_2) \\ &= \frac{1}{Z_0}(0 - 1) \\ &= -\frac{1}{Z_0}, \end{aligned} \tag{16}$$

$$\begin{aligned} H_z &= \frac{1}{Z_0}(V_1 - V_3) \\ &= \frac{1}{Z_0}\left(\frac{1}{2} - \frac{1}{2}\right) \\ &= 0. \end{aligned} \tag{17}$$

Obviously, the Poynting vector is in the positive z direction. Therefore, the difference signal is represented, for each time step k, by a line of impulses weighted by the value of the inverse Fourier transform of $\Phi^{\text{diff}}_{\text{left}}(\omega)$ or $\Phi^{\text{diff}}_{\text{right}}(\omega)$.

Finally, the modified total solution is defined by the following expressions:

$$\phi^{T'}_{\text{left}}(i, k) = \phi^{T}_{\text{left}}(i, k) - \mathcal{F}^{-1}[\Phi^{\text{diff}}_{\text{left}}(\omega)] \tag{18}$$

$$\phi^{T'}_{\text{right}}(i, k) = \phi^{T}_{\text{right}}(i, k) - \mathcal{F}^{-1}[\Phi^{\text{diff}}_{\text{right}}(\omega)] \tag{19}$$

and using (10) and (11)

$$\phi^{T'}_{\text{left}}(i, k) = \phi^{T}_{\text{left}}(i, k) - \mathcal{F}^{-1}[\Phi^{D}_{\text{left}}(\omega) - \Phi^{W}_{\text{left}}(\omega)] \tag{20}$$

$$\phi^{T'}_{\text{right}}(i, k) = \phi^{T}_{\text{right}}(i, k) - \mathcal{F}^{-1}[\Phi^{D}_{\text{right}}(\omega) - \Phi^{W}_{\text{right}}(\omega)]. \tag{21}$$

Fig. 6 shows how the two right-hand terms of (20) and (21) are represented in the TLM network. The first term, $\phi^{T}_{\text{left}}(i, k)$ or $\phi^{T}_{\text{right}}(i, k)$, is the total voltage of the node i at time k, and corresponds to the voltage impulses incident on that node [Fig. 6(a)]. This signal is the total solution obtained by a regular TLM analysis. It contains the dominant and all the higher order modes. But the second term, which is the inverse Fourier transform of the difference signal, contains only a TEM wave (either propagating toward the right or the left). Therefore, the values of the incident impulses describing this signal are equal along the transversal dimension, as shown in Fig 6(b) for the left input.

Finally, the difference between the new total response $\phi^{T'}(i, k)$ and the homogeneous response $\phi^{H}(i, k)$ is reinjected into the empty structure, yielding an image of the synthesized obstacle as described in the previous section. This result represents an improvement over the initial guess, and in

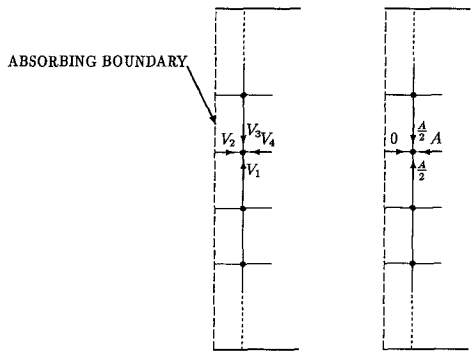

Fig. 6. Nodes adjacent to the left-hand side absorbing boundary. Voltages describing (a) the total response and (b) voltages describing the difference signal.

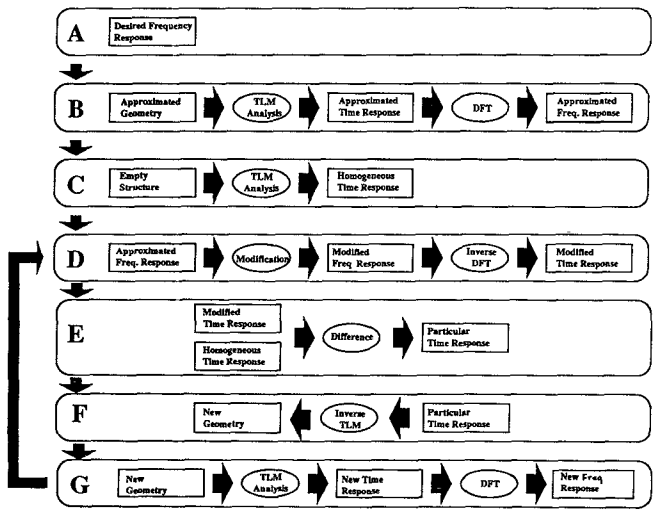

Fig. 7. Flowchart of the proposed synthesis technique.

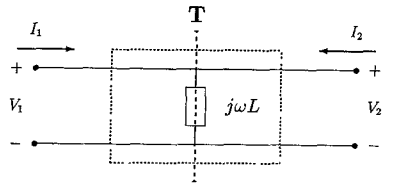

Fig. 8. Representation of an inductor as a two-port network.

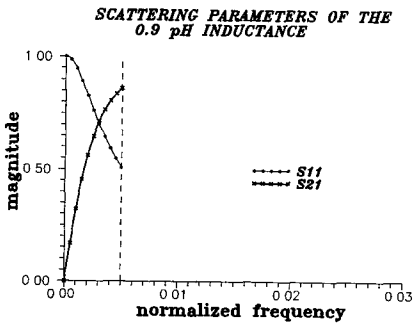

Fig. 9. Specifications for the scattering parameter S_{11} and S_{21} versus the normalized frequency $\Delta l/\lambda$ in the reference plane T. Above 0.005 ($\Delta l/\lambda$), no specifications are given.

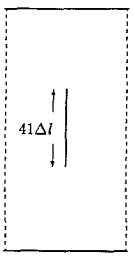

Fig. 10. Configuration of the approximated structure.

many cases, is already acceptable as a final result. However, if a new analysis still yields an unsatisfactory answer, the same sequence is repeated until it converges. Fig. 7 shows a flowchart of this synthesis technique.

B. Numerical Example: Synthesis of an Inductive Obstacle

In this section, a complete design example is presented to demonstrate this novel synthesis technique. The design problem is to synthesize an inductive obstacle in a parallel plate waveguide. Its shunt inductance (see Fig. 8) should be $L = 0.9$ pH within the dominant single mode bandwidth. This design goal leads directly to the desired scattering parameters S_{11} and S_{21} of the obstacle which are shown in Fig. 9, and which we shall call the design specifications.

At this point, the designer has a choice among different configurations which can satisfy these specifications. Among others, a metallic iris, a post, or a septum can be selected. For the present example, a metallic septum is chosen (see Fig. 10). An approximate formula could be used to predict the width for this obstacle, and thus the final result of the synthesis should be close to that value. However, to illustrate the fast convergence of the synthesis procedure, a much larger obstacle of width $41\Delta l$ is chosen as a first guess. The TLM analysis of this structure provides the full bandwidth response in the time domain. A transverse spatial Fourier expansion of this response is used to obtain the impulse response of the structure for the dominant mode which is displayed in Fig. 11. The corresponding frequency domain response is obtained using a discrete Fourier transform (DFT) (see Fig. 12). This frequency response is then modified by substituting, in the low-frequency band, the desired S-parameter values given in Fig. 9, but retaining the higher frequency part. Using an inverse discrete Fourier transform, the modified time domain signal is created. It is used in the reconstruction technique in order to obtain the shape of a new obstacle which corresponds to the design specifications. This new shape is displayed in Fig. 13. It represents an improvement over the original metallic septum. A new analysis shows that this new configuration provides results which agree with the wanted frequency response at low frequencies. The new scattering parameters are displayed in Fig. 14.

V. Discussion

The proposed new technique has shown promising results. But some additional details must be explained. First, if the

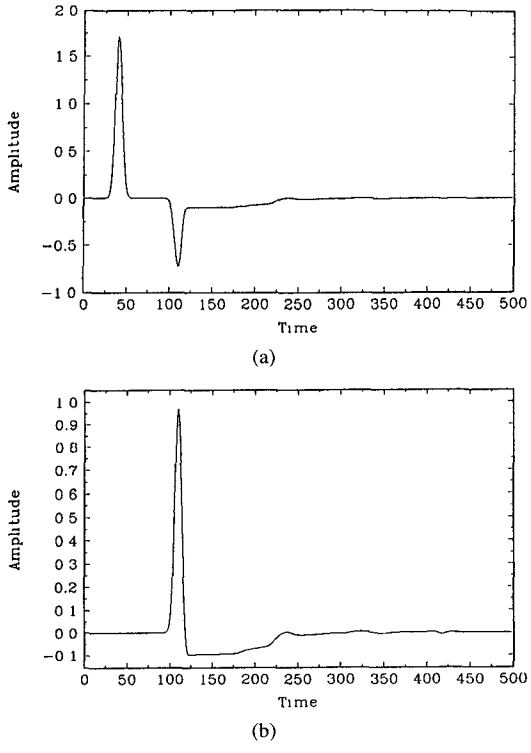

Fig. 11. Impulse responses for the dominant mode (for the electric field E_y) on the left (a) and the right (b) sides of the approximated structure.

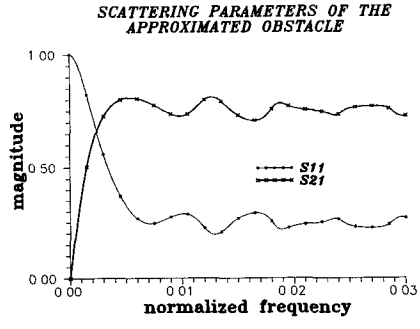

Fig. 12. Scattering parameters of the approximated structure. These are obtained using a discrete Fourier transform (DFT) performed on the approximated time domain signals.

process is followed as described above, only the left part of the obstacle will appear. This is due to the fact that induced sources appear mainly on the left side where the incident wavefront hits. However, a simulation with illumination from the right side can also be performed to get the image of the other part of the obstacle, or both can be combined in a single process involving even excitation from both sides.

Also, current design techniques are based on optimization procedures [5]. Fig. 15 shows a simplified algorithm for such techniques. Usually, the number of variables in optimization procedures must be small to ensure fast convergence of the process. However, the proposed technique is independent of the shape of the obstacle. Thus, for a more complex structure which would require an important number of variables, the

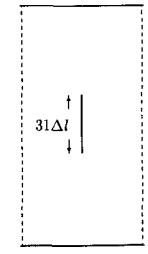

Fig. 13. New configuration of the structure.

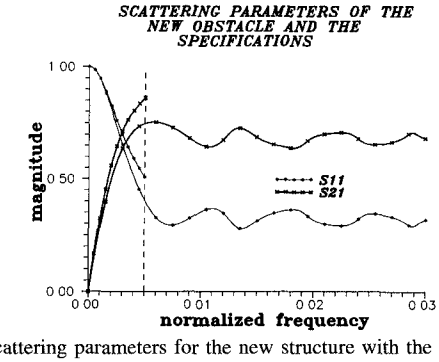

Fig. 14. Scattering parameters for the new structure with the specifications.

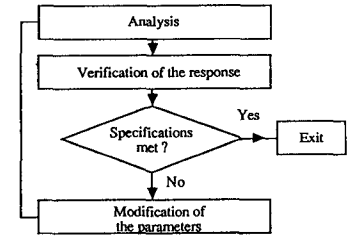

Fig. 15. Flowchart of the traditional synthesis techniques using optimization procedures.

synthesis procedure using time reversal would be more efficient than an optimization procedure. The performance of the new method depends mainly on the mesh density and the quality of the initial guess for the dimensions of the obstacle. Some of the results presented in this paper have been obtained by computation on the Connection Machine, which is a massively parallel computer. Since the TLM scattering computation is identical for each node, it is easy to associate to each available processor one node of the TLM mesh. This makes the TLM method a powerful tool for time domain analysis and synthesis of electromagnetic structures. Finally, the main drawback of this new technique resides in the difficulty of synthesizing resonant structures. In this case, the resonant effect is producing output at both ports for a long time, resulting in a poorly reconstructed image. To be resolved, this interesting problem should be addressed in a future study.

VI. Conclusion

A new technique for the time domain synthesis of microwave structures has been presented. Based on the principles introduced by Sorrentino *et al.* [1], this new efficient algorithm

employing the Transmission-Line Matrix method has yielded good results for simple scatterers inside a waveguide. It has been shown that the required information on higher order modes (which is not provided by the design specifications) can be generated by a forward analysis of an approximated structure. It is at this point that the designer can make a choice among several acceptable solutions. For example, an inductive obstacle could be realized in many possible forms, such as rectangular or circular posts, longitudinal or transverse septa, irises, etc. This distinguishes design from inverse scattering where a specific unknown scatterer must be reconstructed. Future research will be aimed at the development of more general procedures for the synthesis of more complex geometries such as filters, couplers, and hybrid junctions.

ACKNOWLEDGMENT

The authors would like to thank Prof. A. Papiernik and Prof. D. Pompei of the Laboratoire d'Electronique of the Université de Nice, Sophia Antipolis, France, for the opportunity to perform the TLM simulations on their Connection Machine.

REFERENCES

[1] R. Sorrentino, P. P. M. So, and W. J. R. Hoefer, "Numerical microwave synthesis by inversion of the TLM process," in *21st Euro Microwave Conf. Dig.*, Stuttgart, Germany, Sept. 1991, pp. 1273–1277.

[2] P. B. Johns and R. L. Beurle, "Numerical solution of 2-dimensional scattering problems using a transmission-line matrix," *Proc. IEE*, vol. 118, pp. 1203–1208, Sept. 1971.

[3] W. J. R. Hoefer, "The transmission-line matrix method—Theory and application," *IEEE Trans. Microwave Theory Tech.*, vol. MTT-33, pp. 882–893, Oct. 1985.

[4] C. L. Bennet, "Time domain inverse scattering," *IEEE Trans. Antennas Propagat.*, vol. AP-29, Mar. 1981.

[5] M. A. Strickel and A. Taflove, "Time-domain synthesis for broad-band absorptive coating for two-dimensional conducting targets," *IEEE Trans. Antennas Propagat.*, vol. 38, July 1990.

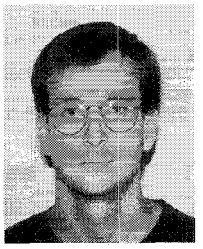

Michel Forest was born in Montréal, P.Q., Canada, on November 17, 1966. He received the B.Ing. degree in electrical engineering from l'Ecole Polytechnique de Montréal, and the M.A.Sc. degree from the University of Ottawa in 1990 and 1992, respectively.

In 1992, he joined the Space Systems Division of Spar Aerospace Ltd., Sainte-Anne-de-Bellevue, Québec. He has been involved in the design, modeling, and testing of beam-forming networks for satellite antennas.

Mr. Forest is a Registered Professional Engineer in the Province of Québec. He received First Prize in the Student Paper Contest at the International Microwave Symposium, Albuquerque, NM, in 1992.

Wolfgang J. R. Hoefer (M'71–SM'78–F'91) received the Dipl.-Ing. degree in electrical engineering from the Technische Hochschule Aachen, Germany, in 1965, and the D.Ing. degree from the University of Grenoble, France, in 1968.

During the academic year 1968–1969 he was a lecturer at the Institut Universitaire de Technologie de Grenoble and a research fellow at the Institut National Polytechnique de Grenoble, France. In 1969 he joined the Department of Electrical Engineering, University of Ottawa, Canada, where he was a professor until March 1992. Since April 1992 he has held the NSERC/MPR Teltech Industrial Research Chair in RF Engineering in the Department of Electrical and Computer Engineering, University of Victoria, Canada, and he is a Fellow of the Advanced Systems Institute of British Columbia. During sabbatical leaves, he spent six months with the Space Division of AEG-Telefunken, Backnang, Germany (now ATN), and six months with the Electromagnetics Laboratory of the Institut National Polytechnique de Grenoble, France, from 1976–1977. During 1984–1985 he was a visiting scientist at the Space Electronics Directorate of the Communications Research Centre, Ottawa, Canada. He spent a third sabbatical year in 1990–1991 as a visiting professor at the Universities of Rome "Tor Vergata" in Italy, Nice—Sophia Antipolis in France, and Munich (TUM) in Germany. His research interests include numerical techniques for modeling electromagnetic fields and waves, computer-aided design of microwave and millimeter wave circuits, microwave measurement techniques, and engineering education.

Dr. Hoefer is the cofounder and Managing Editor of the *International Journal of Numerical Modelling*.